Multichannel Analysis of Surface Waves (MASW) determined surface-wave velocity profile and its relation to observations of the near-surface polar firn layers

Martina Armstrong
GCAS 2008/09

Abstract

A Multichannel Analysis of Surface-Waves (MASW) determined shear-wave (Vs) profile was related to observations of the near-surface polar firn layers on the Erebus Ice Shelf, Ross Island, Antarctica. The surface-wave method (MASW) provides a useful non-invasive tool where information about elastic properties of near-surface polar firn can be effectively obtained. It is not clear at this point if the method can directly determine density variations of the firn without further correlative P-wave or poisons ratio information. The Vs profile obtained shows a general increase in velocity with increasing depth, from 600 m/s at the surface to 1400 m/s at a depth of 12 m. The results indicate that further experiments are likely to yield useful data on the elastic properties of whole firn zone. Recommendations are made regarding equipment set up for further surveys carried out on the Erebus Ice Shelf.

Introduction

Active source body-wave survey methods such as seismic reflection and refraction have been used in glaciological studies for decades. The depth of ice characterised varies from the near surface layers to the base of the ice, which can be up to several kilometres.

Seismic refraction methods have traditionally been used to determine the mechanical properties of shallow snow and ice (e.g. Bentley and Kohnen 1976; Kirchner and Bentley, 1979; Kirchner et al., 1979). Many of the physical processes occurring in a snowpack are intimately tied to the snow's density (Harper and Bradford, 2003). This also influences its mechanical behaviour, as both Young's modulus and viscosity are dependent on density (Mellor, 1975). However, seismic refraction methods are fraught with difficulty in producing shear-waves in firn and also by the presence of dispersed compressional waves interfering with shear-wave arrivals (Tsoflias et al., 2008b).

Standard reflection surveys, which are often used to image the ice-bed interface, contain surface-waves that are typically discarded as noise (Park et al., 1999). In most surface seismic surveys when a compressional wave source is used, more than two-thirds of total seismic energy generated is imparted into Rayleigh surface-waves (Richart et al., 1970), the principal component of ground roll. Rayleigh surface-waves propagate within one wavelength from the surface and their dispersive characteristics can be used to estimate shear-wave velocities (Vs) of the near-surface (Doyle, 1995).

In a study conducted by Tsoflias et al. (2008a), surface-wave data were acquired alongside a conventional-mid-point (CMP) survey line used for deep reflection imaging on the Jacobshavn Glacier, Greenland. The Multichannel Analysis of Surface Waves (MASW) method, which has not been widely used in glaciological research, was then utilised to obtain dispersion curves and estimate the Vs of firn and shallow ice. They found that this method yielded usable dispersion curves and a Vs profile of firn that was consistent with the expected velocity structure in polar regions. The successful results from the study suggest that surface-wave methods can be an efficient alternative to refraction surveys for firn characterisation.

Figure 1: Location of data acquisition on the Erebus ice shelf, Ross Island, Antarctica.

The objectives of this study are to examine the MASW determined Vs profile and relate it to observations of the near-surface polar firn layers. Polar firn is the term given to consolidated snow (King and Jarvis, 2007). The consolidation takes place by a number of processes: by the

reorganisation of grains under the action of gravity and wind redistribution; by pressure melting at grain contacts; and by sublimation and recrystalisation under temperature gradients (Wilkinson, 1988). The density of firn increases continuously from the surface downwards to the point where pore close-off takes place and the material can be considered glacial ice (Herron and Langway, 1980). The study was carried out on the Erebus Ice Shelf, Ross Island, Antarctica at 77°46.543' S, 167°04.449' E (Figure 1).

Method

The geophones, of which there were 24 at 8 Hz with spacing of 1 m were arranged in a straight line, similar to that of the CMP body-wave reflection surveys (Doyle, 1995) (Figure 2). Four MASW shots were gathered. The seismic source used a 10 kg sledgehammer impacting a steel plate. The distance from the source to the first geophone was 10 m. The MASW data was recorded using a Geometrics Stratavisor NX48 Seismograph. When using the MASW method, each channel is dedicated to recording ground roll from one receiver or geophone. One multichannel record (commonly referred to as a shot gather) consists of multiple geophone time series (called traces) from all the receivers in an ordered manner. Figure 3 displays a typical MASW survey set up. The acquisition parameters used for the MASW testing on the Erebus ice shelf were as follows: record lengths set to 1 s (-10 ms pre-trigger delay), no acquisition filters, 0.25 ms sampling interval, only channels 1-24 set active, gains set to 48 dB, 4 stacks (hammer blows 5 s apart), and SEG-2 seismic format.

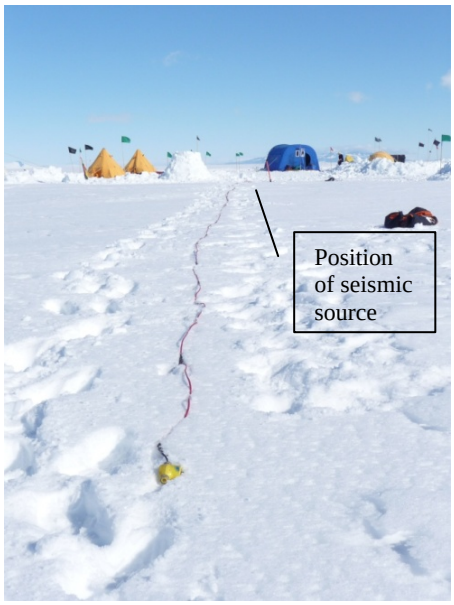

Figure 2: Position of geophone array in relation to the seismic source on the Erebus ice shelf. The image is facing west.

The snow pit of 4.6 m was excavated at the same location (Figure 1). The size and type of snow crystals and the temperatures were recorded in the pit at 20 cm vertical spacing (Appendix 2). At the same sampling interval, the density was determined by firstly weighing a cylinder, containing a known volume of snow, and subtracting the weight of the cylinder. Snow density was then calculated by dividing the weight of the snow by the volume of the cylinder. Photos were also taken up to a depth of 130 cm (Appendix 1). Snow crystal size and type were classified using a chart; however this data is relatively unreliable due to the inexperience of those that were recording it. It must be noted that there was also the potential for error associated with sampling and weighing the volume of snow. The error associated with both of these methods may be as high as 10%.

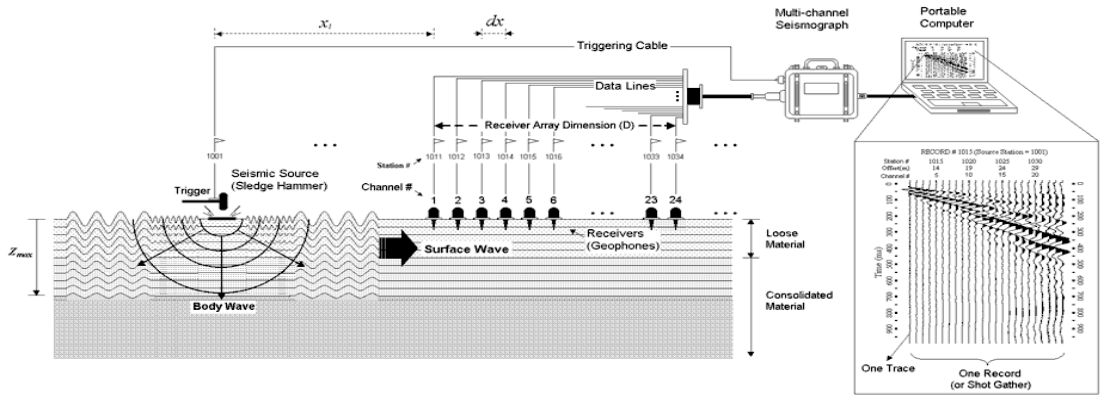

Figure 3: Schematic illustration of a typical Multichannel Analysis of Surface Waves survey set up (KGS, 2007).

Data processing, using Surfseis Software from KGS (2007), consists of three steps (Figure 4):

1) Preliminary detection of surface-waves,

2) Constructing the dispersion image panel and extracting the signal dispersion curve, and

3) Back-calculating Vs variation with depth.

All these steps can be fully automated. The preliminary detection of surface-waves examines recorded seismic waves in the most probable range of frequencies and phase velocities. Construction of the image panel is accomplished through a 2-D (time and space) wavefield transformation method that employs several pattern-recognition approaches (Park et al., 1998). The image panel shows the relationship between phase velocity and frequency for those waves propagated horizontally and directly from the impact point to the receiver line. These waves include fundamental and higher modes of surface-waves as well as direct (compressional) body-waves. The necessary dispersion curve, such as that of fundamental-

mode Rayleigh waves, is then extracted from the energy accumulation pattern in this image panel. The reference point for this was set at a frequency of 30 Hz and a phase velocity of 1300 m/s. The extracted dispersion curve is finally used as a reference to back-calculate the Vs variation with depth below the surveyed area. This back-calculation is called inversion and the process can be automated with reasonable constraints (Xia et al., 1999). Poisson's ratio was altered from the set value of 0.4 to 0.26 as expected for materials with a density of 400 kg m-3 (Kingery, 1963). This value was chosen based on the data obtained from the snow pit.

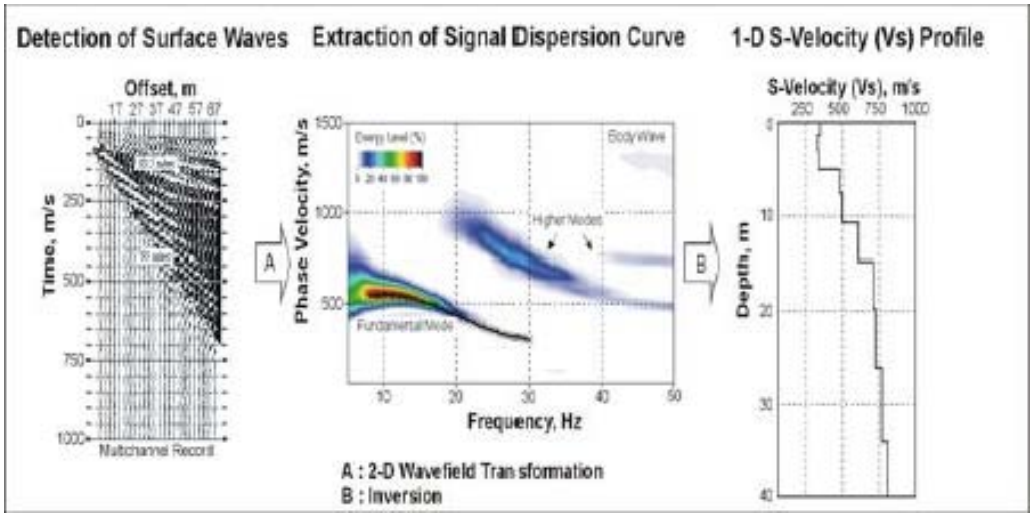

Figure 4: A three-step processing scheme for Multichannel Analysis of Surface Waves data (KGS, 2007).

Results and Discussion

The dispersion curve extracted using the MASW method is in Figure 5 and its associated Vs profile in Figure 6. The resolution of this data is 6 m horizontally and 1 m vertically. Usable data was obtained up to a depth of 20 m. This was much shallower than the previous study that utilised the MASW method on polar firn, conducted by Tsoflias et al. (2008a). They imaged down to 50 m on the Jacobshavn Glacier, Greenland. By doing so, they were able to identify the firn-ice transition; however their detailed analysis of the firn layers was limited.

An increment of 2 m was used in dispersion analysis, as when this was decreased to 0.5 m (Appendix 3, 4, and 5) the Vs profile modelled was not consistent with the expected velocity structure of polar firn. The Vs profile (Figure 6) shows a general increase in velocity with increasing depth, from 600 m/s at the surface to 1400 m/s at a depth of 12 m. Vs can range from under 700 m/s near the snow surface to over 1900 m/s in polar ice (Thiel and Ostenso,

1961). This highlights the relationship between density and velocity, with velocity increasing as density increases. An empirical relationship between p-wave velocity and density was developed by Kohnen (1972). However, no empirical relationship exists for the relationship between density and surface-wave velocity and the MASW software is not capable of deriving such a relationship.

There is an inversion in the Vs profile between 2 and 4.5 m. By reviewing the obtained snow pit data (Appendix 2) the only correlation found with this inversion is with an increase in crystal size. From 1.8 m to 3 m the crystal size recorded was larger than that of the surrounding layers. The reason behind this observed difference may relate to an increase in the initial growth rate of crystals which can often result from the large temperature gradients observed in the top few metres of polar firn (Patterson, 1994). Larger crystal sizes may cause a decrease in Vs, hence explaining the inversion in Figure 6. However this cannot be confirmed.

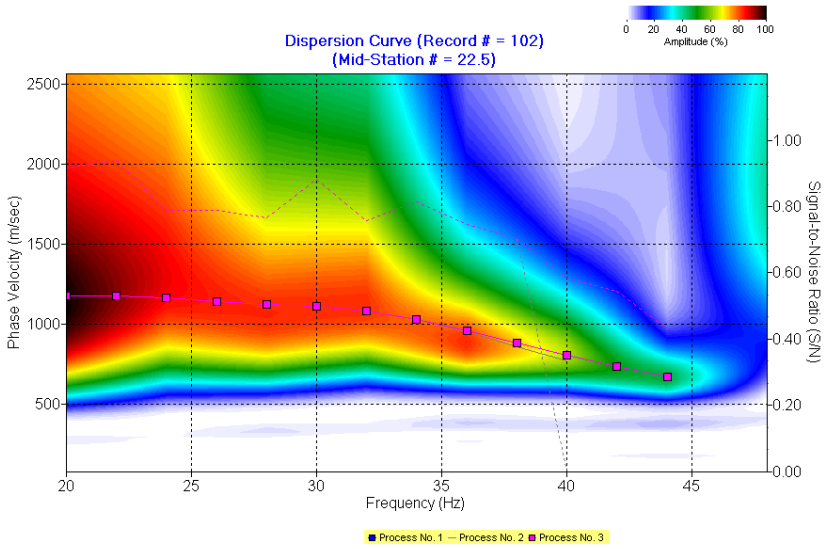

Figure 5: Overtone image showing dispersion curve with an increment of 2.00.

The data obtained from the snow pit (Appendix 2) indicates that there is some variation in density throughout the snow profile, particularly in the top 2.5 m. At the top of the profile, the density is at 330 kg m^{-3} which is just above the range expected for settled snow at 200-300 kg m^{-3} (Petrenko and Whitworth, 1999). This could be a result of compaction related to human activity around the pit edges. The photos in Appendix 1 show ice layers throughout the top 130 cm of the profile which are interspersed with firn layers. These density changes

are irregular on both the vertical and horizontal scale; therefore it can be assumed that the ice layers are discontinuous, localised features.

If these were interpreted as localised areas of melt and refreeze at the surface of the seasonal snowpack, one could use this to indicate that there is variation in snow accumulation on the Erebus Ice Shelf. This is because of the difference observed in snow thickness between the ice layers. This variation could be due to spatial redistribution of snow or seasonal precipitation levels. The ice layers may, however, be a result of downward percolation of meltwater from surface or subsurface melt refreezing to hard layers of large crystals. Therefore it cannot be assumed that these layers are at the top of seasonal accumulation.

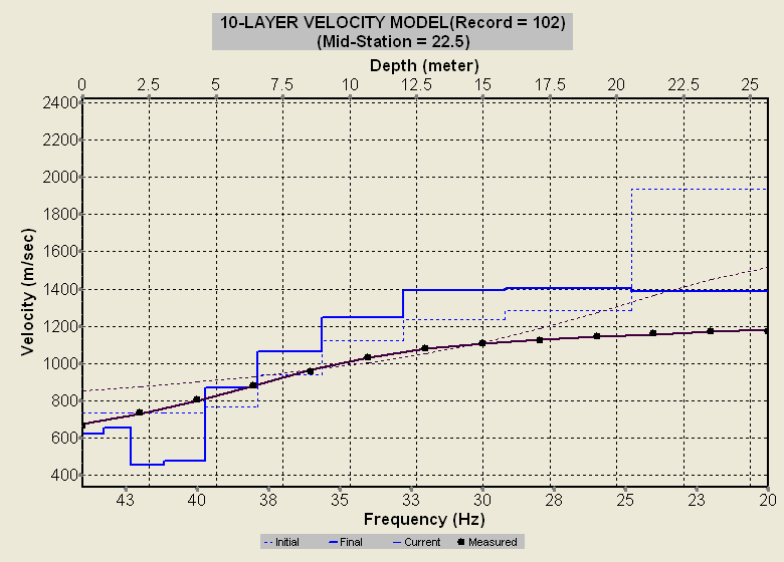

Figure 6: 1D S-Velocity (Vs) profile obtained from the dispersion curve with an increment of 2.00 and with 10 layers.

Dunse et al. (2008) state that the frequency of ice layers is dependent on the cold content of the snowpack. The cold content describes the energy required to heat a unit of snow up to melting point. Due to the temperature in the upper layers of the snow pit ranging from +1 ˚C to -3.8 ˚C (Appendix 2) it can be assumed that the cold content of the snowpack is low. In snowpack of low cold content, serious percolation can lead to extensive ice-layer formation and is likely to affect a greater fraction of the winter accumulation. In the case of high initial snow temperatures and warm summers, extensive breakthrough and limited ice-layer formation results in isolated ice lenses. Due to the coastal position of the Erebus Ice Shelf, high initial temperatures could be expected and relatively warm summers are experienced. This could explain the discontinuous nature of the ice layers. Also, Pfeffer and Humphrey

(1996) state that the majority of refreezing meltwater is expected in the lowermost fraction of the winter accumulation, eventually accreted as thick ice on top of the previous summer surface. Therefore, if this scenario applies to the snow profiles obtained from the Erebus Ice Shelf, the ice layers actually indicate the base of the seasonal accumulation, not the surface.

Snow re-distribution from aeolian processes may also be the reason behind the discontinuous ice layers (Frezzotti et al., 2002). The wind in Antarctica has the capacity to transport large quantities of snow, creating various erosional and depositional surface features. The presence of sastrugi on the Erebus Ice Shelf was observed, indicating that erosional processes were in operation. Sastrugi, along with other factors such as snow impurities, destructive metamorphosis, and decreasing zenith angle, decrease the albedo and enhance surface melt (Frezzotti et al., 2002). Normally, the high albedo of snow cover prevents excessive levels of surface melt. However, due to the decrease in albedo from sastrugi, increased localised melting could occur on these erosional features, giving rise to isolated ice layers. These layers, however, are not presented in detail on the Vs profile (Figure 6). Increasing the amount of layers used in the inversion analysis may enable a more detailed and accurate modelled Vs profile.

Conclusions

The surface-wave method (MASW) provides a useful non-invasive tool where information about elastic properties of near-surface polar firn can be effectively obtained. It is not clear at this point if the method can directly determine density variations of the firn without further correlative P-wave or poisons ratio information. This survey can be considered a pilot study regarding the use of MASW in characterising the physical and mechanical properties of polar firn. The results indicate that further experiments are likely to yield useful data on the elastic properties of whole firn zone.

Further studies using the MASW method on polar firn should experiment with alterations to the equipment set up. Lower frequency geophones, for example, would increase the depth of the Vs profile as it would allow lower frequency surface-waves to be recorded. Using a larger seismic source would generate larger surface-waves which would also produce deeper imaging. A closer spacing between geophones may allow the top 5 m to be characterised in more detail, increasing the vertical and horizontal resolution. In doing so, more accurate

correlations may be made between snow pit and MASW data. More extensive surveys, using a towed array, should be carried out on the Erebus Ice Shelf. This would allow for a more detailed analysis of the spatial variability in both the physical and mechanical properties of polar firn.

References

Alley, R.B. 1988. Concerning the deposition and diagenesis of strata in polar firn. *Journal of Glaciology* 34 (118), 283-290.

Bentley, C.R. and Kohnen, H. 1976. Seismic refraction measurements of internal friction in Antarctic ice. *Journal of Geophysical Research* 81 (8), 1519-1526.

Doyle, H.A. 1995. *Seismology.* Wiley, New York.

Dunse, T., Eisen, O., Helm, V., Rack, W., Steinhage, D. and Parry, V. 2008. Characteristics and small-scale variability of GPR signals and their relation to snow accumulation in Greenland's percolation zone. *Journal of Glaciology* 54 (185), 333-342.

Frezzotti, M., Gandolfi, S., La Marca, F. and Urbini, S. 2002. Snow dunes and glazed surfaces in Antarctica: new field and remote sensing data. *Annals of Glaciology* 34, 81-88.

Harper, J.T. and Bradford, J.H. 2003. Snow stratigraphy over a uniform depositional surface: spatial variability and measurement tools. *Cold Regions Science and Technology* 37, 289-298.

Herron, M.M. and Langway, C.C. 1980. Firn densification – an empirical model. *Journal of Glaciology* 25, 373-385.

Kansas Geological Survey (KGS). 2007. Downloaded on 2nd February 2009. http://www.kgs.ku.edu/software/surfseis/index.html

King, E.C. and Jarvis, E.P. 2007. Use of shear waves to measure poisson's ratio in polar firn. *Journal of Environmental and Engineering Geophysics* 12 (1), 15-21.

Kingery, W.D. (ed.) 1963. *Ice and Snow: Properties, Processes, and Applications.* M.I.T. Press, USA.

Kirchner, J.F. and Bentley, C.R. 1979. Seismic short-refraction studies on the Ross Ice Shelf, Antarctica. *Journal of Glaciology* 24 (90), 313-319.

Kirchner, J.F., Bentley, C.R. and Robertson, J.D. 1979. Lateral density differences from seismic measurements at a site on the Ross Ice Shelf, Antarctica. *Journal of Glaciology* 24 (90), 309-312.

Kohnen, H. 1972. On the relationship between seismic velocities and density in firn and ice. *Zeitschrift fgr Geophysik* 38, 925-925.

Mellor, M. 1975. A review of basic snow mechanics. *IAHS-AISH Publication* 114, 251-291.

Park, C. B., Miller, R. D. and Xia, J. 1999. Multichannel analysis of surface waves. *Geophysics* 64, 800-808.

Park, C.B., Miller, R.D., and Xia, J. 1998. Imaging dispersion curves of surface waves on multi-channel record. *The Society of Exploration Geophysicists*, 1377-1380.

Paterson, W.S.B. 1994. *The Physics of Glaciers*, 3rd ed. Elsevier, Oxford.

Petrenko, V.F. and Whitworth, R.W. 1999. *Physics of Ice.* Oxford University Press, Great Britain.

Pfeffer, W.T. and Humphrey, N.F. 1996. Determination of timing and location of water movement and ice-layer formation by temperature measurements in sub-freezing snow. *Journal of Glaciology* 42 (141), 292-304.

Richart, F.E., Hall, J.R. and Woods, R.D. 1970. *Vibrations of soils and foundations.* Prentice-Hall, Inc.

Thiel, E and Ostenso, N.A. 1961. Seismic studies on Antarctic ice shelves. *Geophysics* 26, 706-715.

Tsoflias, G.P., Ivanov, J., Anandakrishnan, S. and Miller, R. 2008a. Use of active source seismic surface waves in glaciology. *CReSIS.*

Tsoflias, G.P., Ivanov, J., Anandakrishnan, S., Horgan, H., Peters, L., Voigt, D. and Winberry, P. 2008b. Firn and shallow ice profiling at Jakobshavn Glacier using dispersed seismic surface waves. *American Geophysical Union* 89 (53), Fall Meeting.

Wilkinson, D.S. 1988. A pressure-sintering model for the densification of polar firn and glacier ice. *Journal of Glaciology* 34, 40-45.

Xia, J., Miller, R.D., and Park, C.B. 1999. Estimation of near-surface shear-wave velocity by inversion of Rayleigh waves. *Geophysics* 64 (3), 691-700.

Appendices

Appendix 1: Photos taken of the top 130 cm of the snow pit.

		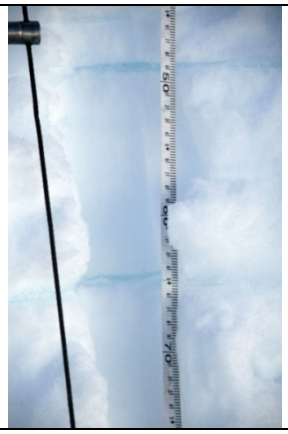
0-30 cm	30-50 cm	50-70 cm
		
70-90 cm	90-110 cm	110-130 cm

Appendix 2: Results obtained from the snow pit. Includes temperature (˚C), density (gm/cc), crystal size (mm), and crystal type.

Depth (m)	Corrected depth (m)	Temp (C)	Weight of snow filled tube (gm)	Density gm/cc	Density kg/m^{-3}	Crystal size (mm)	Type
0	0.1	0.3	150	0.33	330	0.2	F2/1
0.2	0.3	1	140	0.29	290	0.5	F2/3
0.4	0.5	1	160	0.38	380	0.9	F3/2
0.6	0.7	1	150	0.33	330	1	F3/1
0.8	0.9	0.8	140	0.29	290	1.4	F3
1	1.1	-1.9	160	0.38	380	1.2	F3
1.2	1.3	-2.7	150	0.33	330	1.2	F1/3
1.4	1.5	-3.8	170	0.42	420	1.1	F3/1
1.6	1.7	-4.9	157	0.36	360	1.2	F1/3
1.8	1.9	-5	168	0.41	410	1.7	F3/2
2	2.1	-6.5	175	0.44	440	1.6	F1/3
2.2	2.3	-8.1	165	0.40	400	1.8	F3/1

2.4	2.5	-9.5	160	0.38	380	1.6	F3/1
2.6	2.7	-8.1	175	0.44	440	1.5	F1/3
2.8	2.9	-8.5	180	0.47	470	1.5	F1/3
3	3.1	-9.4	180	0.47	470	1.5	F1
3.2	3.3	-10.1	170	0.42	420	1	F1
3.4	3.5	-12.4	170	0.42	420	1	F1
3.6	3.7	-12	180	0.47	470	1	F1
3.8	3.9	-13.1	180	0.47	470	1	F1
4	4.1	-16.1	180	0.47	470	1	F1
4.2	4.3	-16.8	178	0.46	460	1	F1
4.4	4.5	-18	175	0.44	440	1	F8
4.6	4.7	-19	178	0.46	460	2	F1

Appendix 3: Overtone image showing dispersion curve with an increment of 0.5.

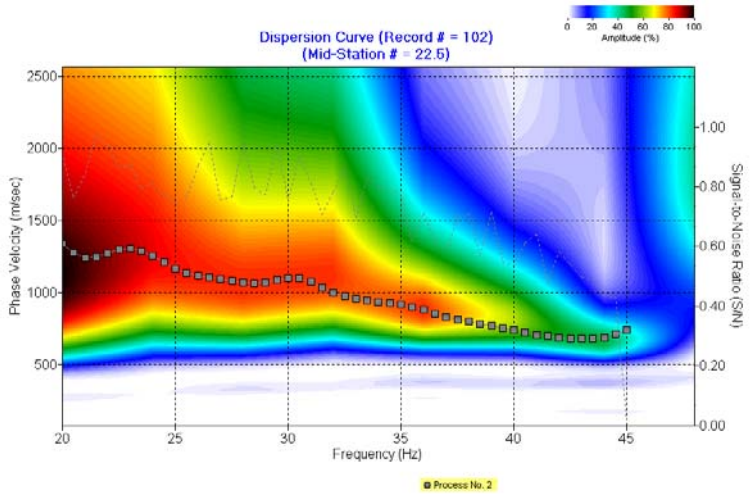

Appendix 4: 1D S-Velocity (Vs) profile obtained from the dispersion curve with an increment of 0.5 and with 20 layers equally spaced.

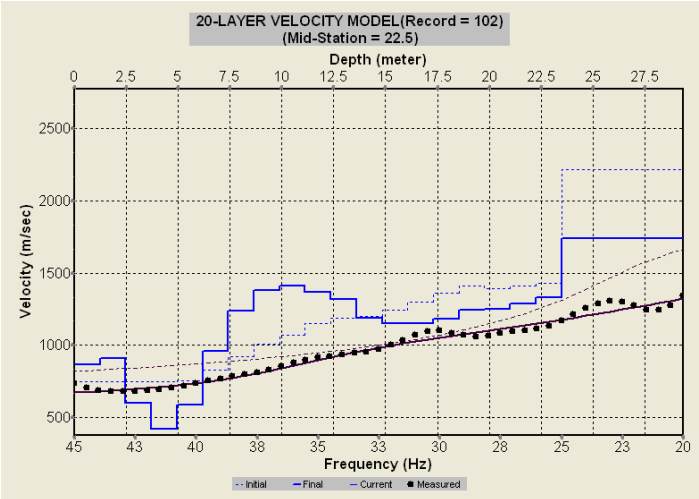

Appendix 5: 1D S-Velocity (Vs) profile obtained from the dispersion curve with an increment of 0.5 and with 10 layers.